BULLETIN OF THE POLISH ACADEMY OF SCIENCES
TECHNICAL SCIENCES, Vol. 61, No. 2, 2013
DOI: 10.2478/bpasts-2013-0030

Hybridization of the lithium energy storage for an urban electric vehicle

M. MICHALCZUK*, L.M. GRZESIAK, and B. UFNALSKI

Institute of Control and Industrial Electronics, Warsaw University of Technology, 75 Koszykowa St., 00-662 Warsaw, Poland

Abstract. This paper discusses benefits of introducing an ultracapacitor (UC) bank into a battery electric vehicle (BEV) powertrain. The case of 12kWh $LiFePO_4$ battery pack is studied quantitatively. Simulation results refer, inter alia, to three main scenarios: fresh cells, half-used battery cells, and half-used ultracapacitors and batteries. Thermal modeling is incorporated into the simulation. Data from real world are considered: various driving cycles recorded using GPS receiver (incl. elevation), discharge curves from battery manufacturer, and UC equivalent series resistance (ESR) variations due to cycling according to real data reported in papers. Cost, as well as gravimetric and volumetric issues are presented. The key decisions referring to an energy storage for BEV being currently designed within the frame of ECO-Mobility Project are highlighted.

Key words: lithium energy storage, ultracapacitors, hybrid energy storage, battery electric vehicle.

1. Introduction

Electrification of urban vehicles is perceived nowadays as an effective solution to personal transportation. It reduces pollution within the cities. The battery electric vehicle (BEV) is called zero-emission one due to no exhaust fumes emission and significant acoustic noise emission reduction – and from this point of view it can be regarded as the environmentally friendly solution. Nevertheless, one should be aware that in many countries energy consumed by BEVs is produced in conventional power plants. Additionally, a worn-out battery is a waste which is energy consuming in utilization. At the same time battery pack is the most expensive part of a typical city car. It is common that the traction battery pack for an A-segment car contributes even one third to its price. Electrical powertrain has enabled engineers to reduce mechanical part of the propulsion system to minimum. Moreover, the electric motor outdoes ICE (Internal Combustion Engine) in terms of torque-speed mechanical characteristics. Hence, it is forecasted that this type of propulsion will be becoming more and more popular in urban vehicles. This trend will be additionally amplified by growing oil prices, which seems inevitable according to all proposed models [1]. The most optimistic estimations of peak oil production forecast undulating plateau to appear after 2030 [2].

Nowadays lithium-based batteries seem to be the most promising energy source/storage for BEVs [3, 4]. However, a cycle life offered by state-of-the-art batteries is still much below typical customer expectations and much below an average life span of ICEV (ICE Vehicle), i.e. 10–15 years. Performance of BEV with electrochemical battery deteriorates with number of charge-discharge cycles and with low temperature. Battery ageing processes result in reduced capacity and power. Many obstacles to BEV commercialization have been already overcome. For example, the problem of the limited range of BEV was solved by introducing EREV (Extended Range EV) being a series plug-in HEV with all-electric mode capability, e.g. Chevrolet Volt and Opel Ampera. In some BEVs all-season capability is maintained thanks to additional heat generators, e.g. Volvo C30 BEV. Other producers have decided to power the HVAC (heating, ventilation, and air conditioning) system for cabin and battery from the traction battery. During cold days this significantly reduces a vehicle range. At 0°C a typical A- or B-segment BEV uses up nearly half of stored energy for heating [5] if not equipped with auxiliary liquid-fuel-operated heat generator. This in turn doubles number of battery cycles needed to cover the same distance and shortens battery life expressed in distance units. Nevertheless, even such range reduced due to HVAC system can be satisfactory for most commuters. For example, it is estimated that in Europe 80% of trips are less than 25 km [4]. According to the U.S. Bureau of Transportation Statistics an average commute from home to work takes less than 30 minutes and only ca. 10% are longer than 50 km [6]. This clearly indicates that BEV can be a reasonable choice as a second car in a household for majority of commuters. According to many reports based on statistical research carried in U.S., Europe and Japan, it is not the limited range that triggers customer's reluctance to buy a BEV. The most important obstacle is still price of an energy storage. Producers estimate that in the near-term mass-produced high-volume battery packs could be available at 300 USD/kWh. A city BEV consumes ca. 0.15 kWh/km. That is why producers usually limit BEVs range to levels far below the ones available for ICEVs. Moreover, todays lithium-ion battery chemistries offer cycle life and calendar life much below customer expectations. If assumed that BEV should operate statistically as long as ICEV, one will be forced to buy a spare battery pack at least once.

*e-mail: marek.michalczuk@ee.pw.edu.pl

Within the ECO-Mobility Project a multidisciplinary team from the Warsaw University of Technology has been designing a city car suitable equally for disabled, elderly and fit people. Electric propulsion with motors moved to wheels and drive-by-wire solutions are of crucial importance in this concept. Flexible interfaces and a flat thin floor are key features that will enable wheelchair users getting in and out without the necessity to transfer from and back to a wheelchair. Affordability of the car and its longevity is one of our main concerns. It is planned to introduce this car as a rent one for urban areas. Due to space and cost concerns nominal capacity of a battery pack has been limited to 12 kWh (40 Ah at 300 V). Nowadays cell chemistries are designed as high-power or high-energy ones. The former are dedicated to experience shallow discharge/recharge cycling in ICE-HEVs. They are characterized by high specific power (even above 1 kW/kg) and relatively high price per kWh. The latter are designed to serve as energy storages for BEVs and are characterized by high specific energy, in some cases at the cost of specific power (even below 0.1 kW/kg). The $LiFePO_4$ cells earn their popularity because of good safety and moderate price. It is typical for most solutions based on $LiFePO_4$ chemistry that cycle life deteriorates significantly if high currents (above 0.5 C-rate) are forced. Their calendar life is reported as poor if operated over 30°C. Note that HVAC system can maintain desired cell temperature in steady states of the vehicle. During acceleration and recuperative braking temperature inside the cell will temporarily rise. Due to the nature of involved chemical reactions power density decreases significantly with falling temperature. The efficiency of a kinetic energy recovery process drops. A lack of sufficient power density needed for maintaining desire vehicle dynamics manifests itself especially if the battery pack has low capacity (like in our design) and required power demand can be covered only at temperatures higher than certain level (e.g. 5°C). In some designs this discrepancy between needed capacity and required power is so strong that the presence of an additional energy storage (high-power storage) is inevitable. It is obvious that supporting any kind of electrochemical battery with high-power storage (e.g. ultracapacitor bank, flywheel system) will extend traction battery lifetime. In such a hybrid-source system the high-energy source covers demand for average power whereas the high-power storage covers energy demand in transient states (acceleration and regenerative braking). If the high-power storage has better discharge-recharge process efficiency than the high-energy primary source, which is typical, the range of a vehicle will naturally extend and this effect will be stronger for heavy traffic conditions. Thus the ultracapacitors (UCs), as the way to improve the performance of lithium battery based storages, are already incorporated into drive systems for public transport, e.g. in plug-in hybrid city buses [7].

Our primary goal is to analyze quantitatively benefits of hybridization of the 12kWh $LiFePO_4$ energy storage with the help of UC bank. There are four case studies presented here: the first one for a fresh battery pack with nominal parameters, the second one with a half-used battery (i.e. having 90% of the nominal capacity) and a fresh UCs, the third one for a half-used battery and a half-used UCs, and the fourth one for a fresh battery and a half-used UCs. The two last case scenarios happen when used battery is replaced with a new one. Typical UCs with 10^6 cycles capability should provide calendar life of an auxiliary storage comparable to vehicle calendar life. Our simulation study is focused on vehicle range in various temperature conditions (no battery powered HVAC for cabin is assumed). The packaging (i.e. volume and mass) issues are also addressed. It should be noticed that the discussion refers to the commercially available off-the-shelf battery and UC cells. One should be aware that there is a lot of research ongoing in the field of materials (incl. nanomaterials) for batteries and UCs. The commercialization of these solutions will probably change many design approaches to hybrid and non-hybrid energy storages for EVs. The research in this field is stimulated by emerging market of EVs. Researchers already succeeded in introducing nanotechnology into UCs and battery cells [8–12]. It is estimated that in the mid-term UCs could be even taken into account as a primary source for low-range vehicles. New electrolytes are being developed to increase durability and decrease cost of the lithium cells [13].

2. Topologies of HES

The hybrid energy storage (HES), being under consideration as a potential choice for a city car, is an extension of a basic energy storage composed of a battery pack and a bidirectional step-up converter. The step-up converter interfaces battery and enables battery's 250–350 V to be boosted up to 600 V. An additional high-power UC storage is incorporated into this scheme. There are many possible ways to combine batteries and UCs into the hybrid storage. In this section basic topologies of the hybrid systems are presented.

In the simplest configuration both energy storages are directly connected in parallel [14–16]. The main drawback of a passive hybrid is uncontrolled power distribution between both storages. The same terminal voltage of storage components results in power distribution between them determined solely by their instantaneous internal resistances. In addition, energy stored in UCs is proportional to squared voltage, whereas battery's voltage usually varies not so significantly with SOC (state of charge) and for lithium chemistries is relatively flat. This results in low utilization ratio of UCs.

An enhancement of the passive topology are semi-active hybrids, which allow to manage power flow between two energy storages. One instance of the semi-active hybrid is shown in Fig. 1 [17–20]. This topology allows direct exchange of energy between the load and UCs without the use of converter and improves the efficiency of energy recovery. This kind of a semi-active hybrid is favorable in case of pulse loads like in portable electronic devices. If incorporated into BEV powertrain, it limits usable capacity of UCs. The minimum allowable voltage of discharged UCs must be higher than the BEMF (back electromotive force) of drive motors at maximum speed. This in turn forces us to use high voltage UC storage, what is less effective, because of the usage of smaller cells, which have worse properties (higher ESR).

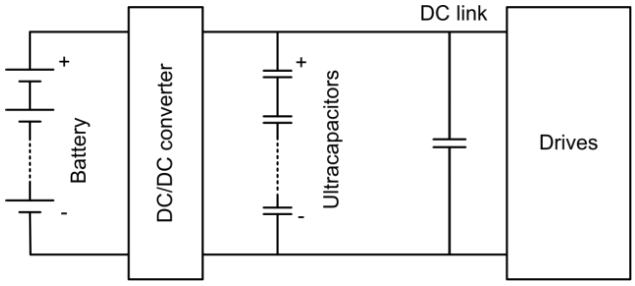

Fig. 1. Powertrain with battery semi-active hybrid

In an alternative semi-active topology (Fig. 2) the additional storage is connected to the battery through a bidirectional DC-DC converter [17, 19]. The battery is connected directly to a load, so there is a need to conform battery's voltage to usually high input voltage of a drive inverter (due to obvious current value concerns systems at the level above 10 kW are usually designed as 300 V and above ones). The nominal battery voltage must be oversized due to terminal voltage variations resulting from low temperatures, high power peaks and low SOC.

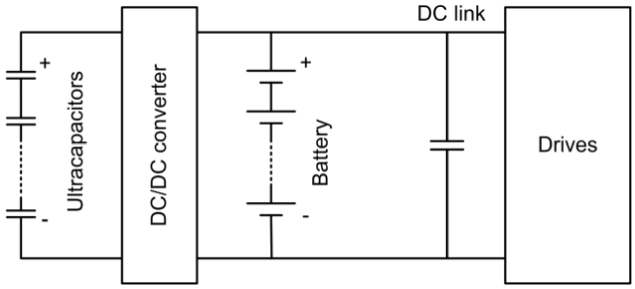

Fig. 2. Powertrain with ultracapacitor semi-active hybrid

Fully active hybrids are free of above-mentioned drawbacks at the cost of second converter. Figure 3 shows an active cascaded hybrid topology whereas Fig. 4 shows a parallel active hybrid topology [14, 16, 17, 19, 21]. Two DC/DC converters solve the problem of matching the voltage of sources to the BEMF. Additionally, in the fully active hybrid systems there is no need to size the converter associated with the battery for high power peaks. The main deficiency of the cascaded topology is that energy delivered from the battery is flowing through both converters decreasing overall efficiency of the powertrain. The parallel active topology with two bidirectional converters has been selected for implementation in this research.

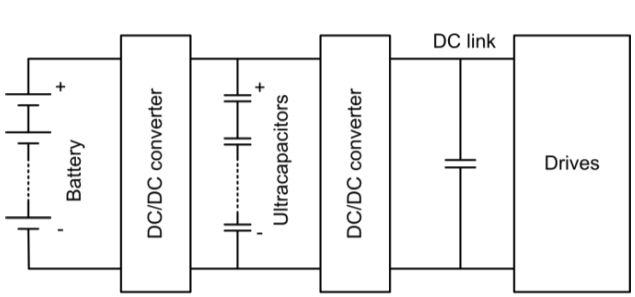

Fig. 3. Powertrain with fully-active cascaded hybrid

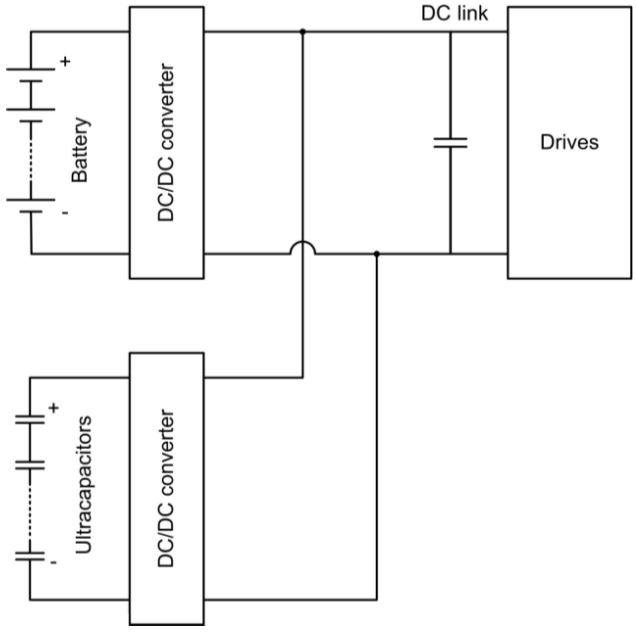

Fig. 4. Powertrain with fully-active parallel hybrid

3. Power management strategies for HES

In the discussed powertrain for a city car the battery storage is handled as a low-power high-energy one to extend its lifespan. Supporting UCs serve as a high-power low-energy auxiliary storage. Thus, the battery should cover average power demand and UCs should be engaged during high power loads and regenerative braking. A basic control strategy limits power provided by the battery and below certain threshold the battery works unaided. When demanded power crosses the threshold, the UC starts to discharge. High limit results in a rare use of the UC. On the other hand, low limit can cause discharging of the UCs at high speeds due to growing air drag force. Minimization of the additional cost introduced by an auxiliary storage can be achieved by appropriate power distribution between storages depending on instantaneous power demand, instantaneous speed of a vehicle and a state of charge of UCs.

The main idea of power distribution is shown in Fig. 5. Under constant speed and UCs' voltage within desired range, being the function of vehicle instantaneous speed, only the battery is being discharged (state 1). In dynamic state during acceleration (state 2) both storages are discharged simultaneously – the UC takes the power peaks. In order to balance UCs' state of charge, all energy from regenerative braking is captured by UCs (state 3). During the stop additional storage is recharged from battery if needed (state 12). An example of the power-time graph that includes these states is shown in Fig. 6.

In the situation when UCs have reached maximum or minimum state of charge, respectively consecutive charging or discharging is impossible (states 4 and 5). This, in turn, means that the system operates as a non-hybrid one (Fig. 7). In order to avoid such a situation that all power in the dynamic states is provided solely by the battery, appropriate level of UCs'

voltage should be determined as a function of instantaneous speed. The control algorithm calculates the lower value of the reference UCs' voltage that ensures reserve of energy to accelerate to maximum speed. In accordance with equation (1) this value depends on instantaneous speed. If UCs' voltage exceeds lower reference value, discharge is partly abated.

$$U_{ref\_down} = \sqrt{U_{\min}^2 + \frac{m\left(v_{\max}^2 - v^2\right)}{C\eta_1}}, \tag{1}$$

$$U_{ref\_up} = \sqrt{U_{\max}^2 - \frac{mv^2\eta_2}{C}}, \tag{2}$$

where C – capacity of UCs, $U_{\max}$, $U_{\min}$ – maximal and minimal voltage of UCs allowed, m – vehicle mass, v – vehicle instantaneous speed, η_1, η_2 – efficiencies of boost and recovery modes, $v_{\max}$ – maximum speed. In general, η_1 and η_2 depend on deceleration and acceleration over time curves. They also should take into account external forces, e.g. air drag. The simplest approach is to set both of them to 1. One could also set them according to the worst case scenario. In our study it was assumed that they are equal to 1 and 0.55 respectively. Relatively low recovery mode efficiency takes into account friction brakes assistance.

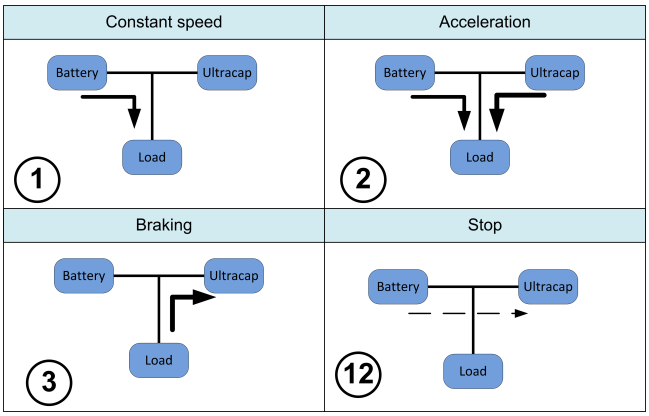

Fig. 5. Energy flow diagrams at nominal states

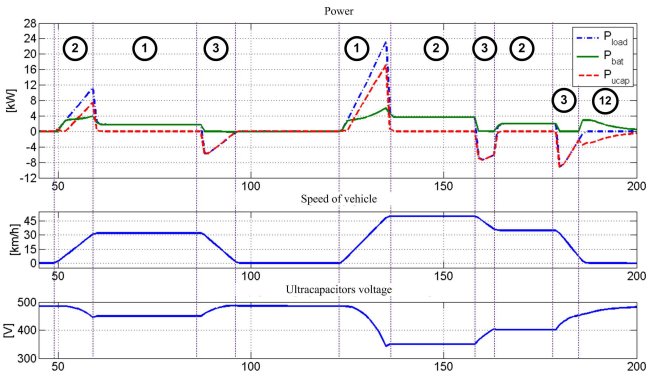

Fig. 6. Power distribution in HES

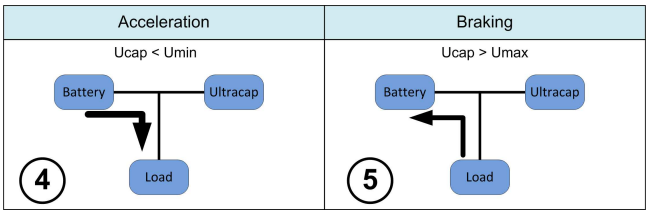

Fig. 7. Energy flow diagrams in no-hybrid state

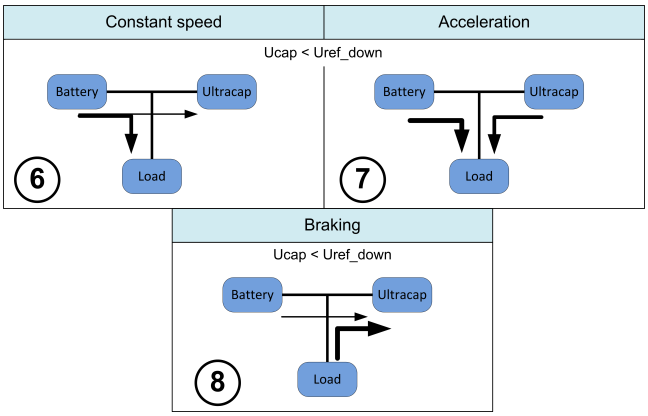

Fig. 8. Energy flow diagrams at low speed and low SOC of ultracapacitor

Figure 9 illustrates driving uphill, so power demand increases. In the period between 320 and 330 second, during acceleration UCs' voltage has exceeded lower reference value and the battery instantaneous power is increasing moderately (state 7 from Fig. 8). This allows to support the battery, at least partially, till the end of acceleration process. Otherwise, the UC would be discharged to its allowed minimum and peak power of 28 kW would have to be provided by the battery. In this particular case the control depending on vehicle speed limits power drawn from the battery down to 14 kW.

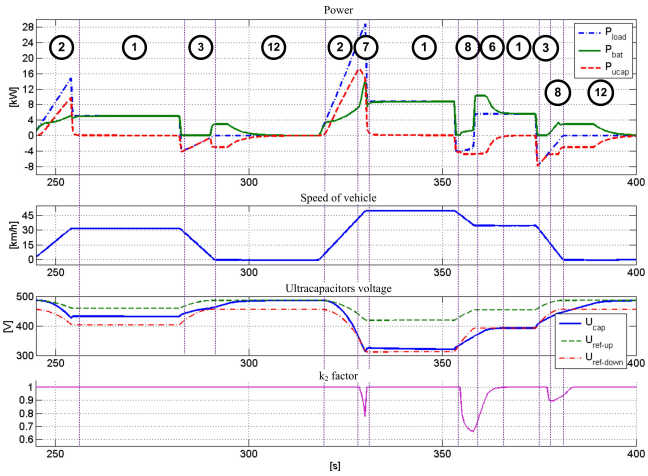

Fig. 9. Power distribution in driving uphill

Similarly to the previously described states, the upper value of the reference UCs' voltage is determined according to (2), which provides an ability to recover energy from braking (Fig. 10). Driving downhill reduces power demand from

the source. A suitable hill steepness allows even to recharge the main energy storage (Fig. 11). Due to the relatively high speed and high SOC of UCs, in the period between 450 and 475 second, energy from regenerative braking (related to downhilling) is primarily captured by the battery. This allows to limit battery instantaneous power during next braking phase (475 s).

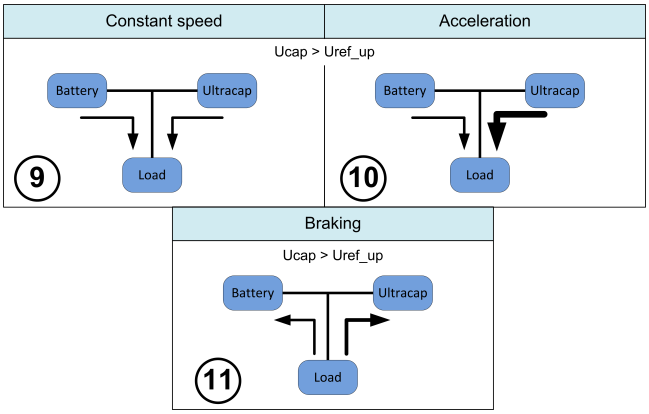

Fig. 10. Energy flow diagrams at high speed and high SOC of ultracapacitor

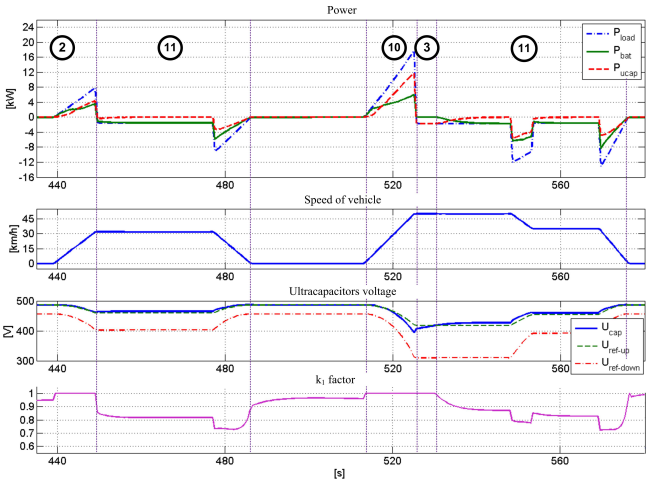

Fig. 11. Power distribution in driving downhill

A schematic representation of the control system is shown in Fig. 12, while more detailed information on control strategy is provided in Fig. 15. There are two inner current control loops associated with two converters. Maintaining desirable voltage of intermediate circuit and UCs as well as appropriate power distribution is achieved by proper reference current value determination. All related to this formulas are given in Table 1. During kinetic energy recovery, the reference current value is proportional to the control error of voltage in the intermediate circuit. Power drawn from the auxiliary energy storage is determined by the coefficient k_1, which value depends on the state of charge for UCs (Fig. 13). In discharge states, battery reference current is proportional to voltage control error for common DC link, while UCs reference current is calculated by means of high-pass filter (HPF) according to equation (3) and is scaled by k_2 factor (Fig. 14). Note that reference values are modified if the threshold U_{ref_down} or U_{ref_up} is exceeded.

$$I_{Load\_HPF}(s) = \begin{cases} (I_{Load} - I_{thold}) \cdot \dfrac{\tau \cdot s}{\tau \cdot s + 1} \\ \qquad \text{for} \quad (I_{Load} - I_{thold}) > 0 \\ 0 \qquad \text{for} \quad (I_{Load} - I_{thold}) \leq 0 \end{cases} \tag{3}$$

where I_{thold} denotes the threshold value for activation of the filter, and τ was set to 20 seconds.

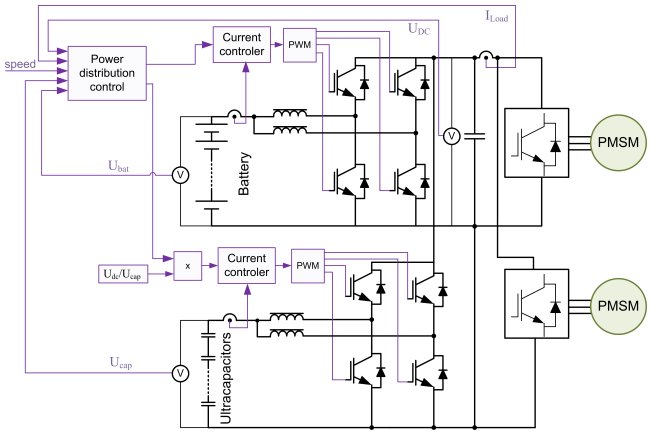

Fig. 12. Control scheme for the hybrid energy storage

Table 1
Reference value calculation

Condition	Reference Value	State (Fig. 5, 7, 8, 10)
$I_{Load} \geq 0$	$I_{ref\_cap} = k_2 \cdot I_{Load\_HPF}$ $I_{ref\_bat} = (600 - U_{DC}) \cdot Kp_1$	3 if $k_1 = 1$ 5 if $k_1 = 0$ 11 if $k_1 \in (0, 1)$
$I_{Load} < 0$	$I_{ref\_cap} = k_1 \cdot (600 - U_{DC}) \cdot Kp_2$ $I_{ref\_bat} = (1 - k_1) \cdot (600 - U_{DC}) \cdot Kp_1$	1, 2 if $k_2 = 1$ 4 if $k_2 = 0$ 6, 7 if $k_2 \in (0, 1)$
$U_{cap} < U_{ref\_down}$	$I_{ref\_cap} = I_{ref\_cap} - (U_{ref\_down} - U_{cap}) \cdot Kp_3$	6, 7, 8
$U_{cap} > U_{ref\_up}$	$I_{ref\_cap} = I_{ref\_cap} + (U_{cap} - U_{ref\_up}) \cdot Kp_4$	9, 10, 11
$v = 0$, $U_{cap} < U_{ref\_up}$	$I_{ref\_cap} = (U_{cap} - U_{ref\_up}) \cdot Kp_5$	12

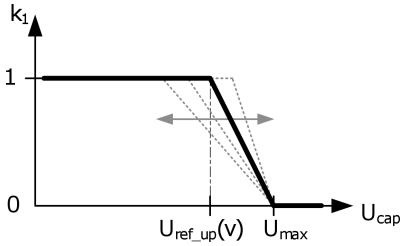

Fig. 13. Factor k_1 as a function of ultracapacitors' voltage (the slope changes with the speed

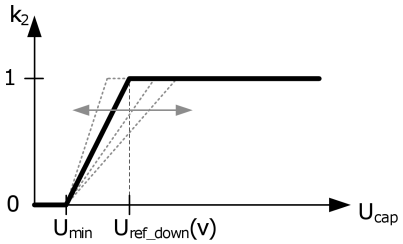

Fig. 14. Factor k_2 as a function of ultracapacitors' voltage (the slope changes with the speed)

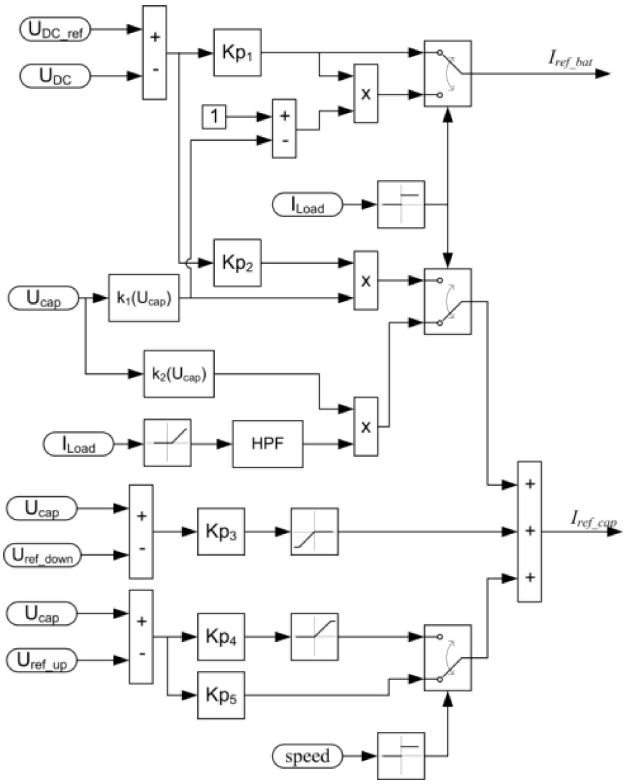

Fig. 15. Block diagram of the control system

4. Simulation model and results

The dynamic characteristics of the battery pack are implemented by means of the Thevenin-based model [22–24] shown in Fig. 16. A voltage source corresponds to the open circuit voltage of the battery. A resistor R_s connected in series with a parallel RC branch models an ohmic drop and polarization effect [22, 23]. A discharge capacity and internal resistance variations resulting from change in discharge current and temperature are modeled as in [25]. Presented model is extended by adding dynamic thermal modeling. This model assumes a uniform temperature for all cells.

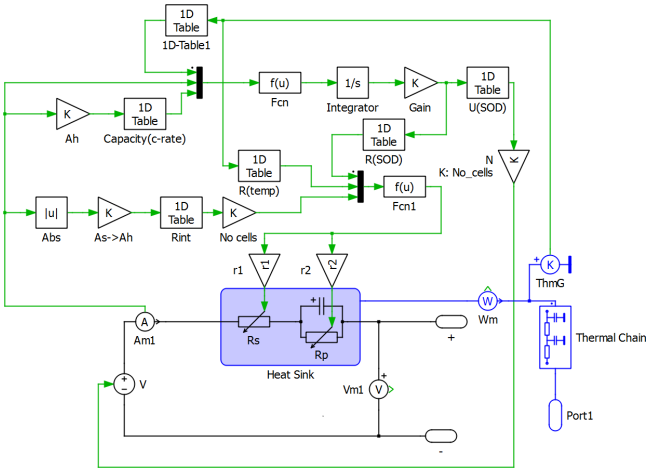

Fig. 16. Battery model (incl. thermal model)

The ultracapacitor model includes an internal resistance R_{ESR} and a voltage controlled source to represent variable capacitance. The implemented model does not take into account a transient voltage change in dynamic states, but is still sufficient to evaluate power losses [25].

A continuous model of the converter was implemented at this stage of simulation. An IGBT+D power losses were calculated based on Eqs. (4)–(11) and Semikron SKM300GB12T4 module parameters given in [26]. Estimates of power losses for continuous model can be few percent higher due to calculations based on an average current, thus not taking discontinuous conduction mode into account. Results from both models were compared. Difference between discontinuous and continuous models in estimation of converter's average power losses occurred to be at the negligible level. It is to notice that simulating e.g. 3000 seconds of converter operation if implemented as discontinuous model (as in Fig. 20) running with e.g. 10 kHz modulator, cannot be done in a reasonable wall-clock time.

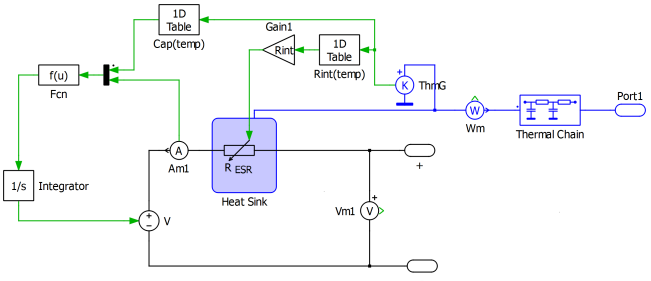

Fig. 17. Ultracapacitor model (incl. thermal model)

Losses per transistor:

$$P_{cond\_tr} = D \cdot (I_{tr} \cdot V_T + I_{tr}^2 \cdot r_T), \tag{4}$$

$$E_{sw} = E_{on} + E_{off}, \tag{5}$$

$$P_{sw\_tr} = f_{sw} \cdot E_{sw} \cdot (I_{tr}/I_{rated}) \cdot (V_{tr}/V_{rated}), \tag{6}$$

$$P_{tr} = P_{cond\_tr} + P_{sw\_tr}. \tag{7}$$

Losses per diode:

$$P_{cond\_d} = (1 - D) \cdot (I_d \cdot V_T + I_d^2 \cdot r_T), \tag{8}$$

$$P_{sw\_d} = f_{sw} \cdot E_{rr} \cdot (I_d / I_{rated}) \cdot (V_d / V_{rated}), \tag{9}$$

$$P_d = P_{cond\_d} + P_{sw\_d}. \tag{10}$$

Total losses:

$$P_{tot} = P_{tr} + P_d, \tag{11}$$

where D – duty cycle, I_{tr} – transistor current, I_d – diode current, I_{rated} – rated current, V_{tr} – transistor voltage, V_d – diode voltage, V_{rated} – rated voltage, V_T – threshold voltage, E_{off} – energy dissipation during turn-off time, E_{on} – energy dissipation during turn-on time, E_{rr} – energy dissipation during reverse recovery (diode), r_T – forward slope resistance, f_{sw} – switching frequency.

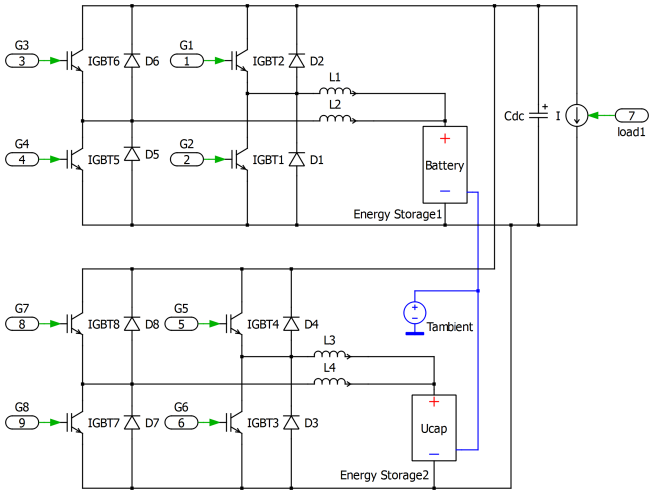

Fig. 18. Active hybrid energy source built for comparison purposes

Table 2
Model parameters

	Battery	Ultracap.
Nominal voltage	295 V	485 V
Min. voltage	257 V	310 V
Capacity of a cell	40 Ah	310 F
Number of cells	92	180
Stored energy	12 kWh	0.056 kWh
Heat capacity	1500 J/K	60 J/K
Thermal resistance	1.44 K/W	10.9 K/W
	Vehicle	
Mass	1200 kg	
Aerodynamic coefficient – C_x	0.37	
Powertrain average efficiency (drive converter and motor)	85%	
Rolling friction coefficient	0.012	
Max. power of drives	35 kW	
Max. acceleration	3 m/s^2	
Max. deceleration	-5 m/s^2	

Table 2 presents parameters of a hybrid energy storage applicable in a small electric car dedicated for urban areas. Such an energy storage provides ca. 140 km of maximal driving range for the car in nominal conditions if high DoD (depth of discharge) is assumed. If DoD limit is set to e.g. 70%, the driving range drops to ca. 100 km. A range like this is still acceptable for such a vehicle if the design is aimed at commuters.

Several comparison tests of the non-hybrid lithium battery source and described hybrid source were carried out. Three reference driving cycles (Figs. 19–21) were taken into account: the normalized European driving cycle ECE15 and two real cycles recorded in the urban area (Warsaw) and in the uplands suburban areas (Bielsko-Biała, Szczyrk). Profiles of speed and terrain were recorded using GPS receiver with sample time less than 2 seconds. A slope in sequence of 0, 1°, $-1°$ changing every 1 km has been added in ECE15 driving cycle.

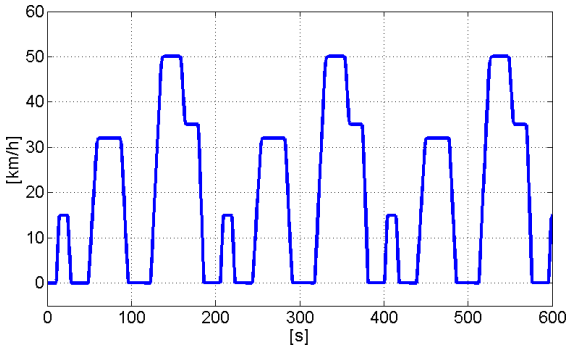

Fig. 19. Normalized driving cycle ECE15

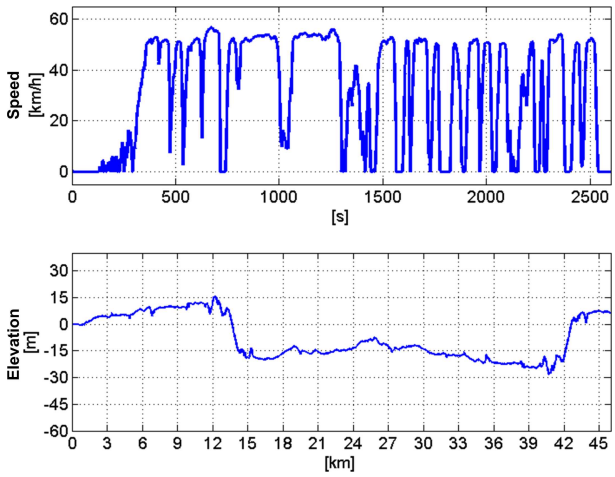

Fig. 20. Real cycle recorded in Warsaw

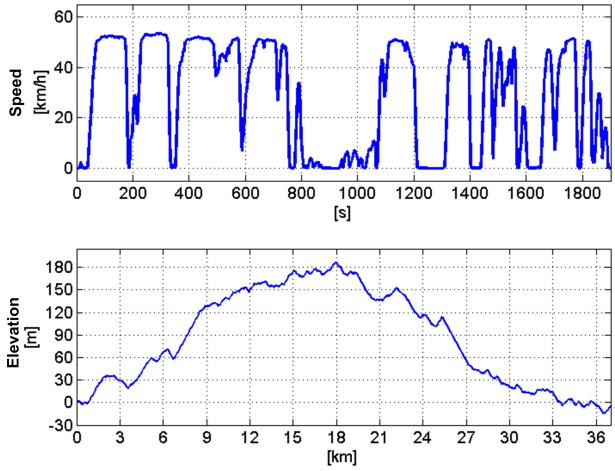

Fig. 21. Real cycle recorded in Bielsko-Biała

Table 3
Simulation result in case of fresh battery cells

		ECE15			Real cycle 1 (urban area)			Real cycle 2 (suburban area)		
		Battery	Hybrid (fresh UC cells)	Hybrid (half-used UC cells)	Battery	Hybrid (fresh UC cells)	Hybrid (half-used UC cells)	Battery	Hybrid (fresh UC cells)	Hybrid (half-used UC cells)
25°C	Range [km]	151.45	164.45	163.59	141.39	149.92	149.77	143.31	148.62	148.54
	Efficiency	95.29%	97.11%	96.89%	95.21%	96.70%	96.54%	94.96%	96.49%	96.36%
10°C	Range [km]	136.89	157.35	157.33	134.81	143.9	141.17	126.28	133.61	133.6
	Efficiency	94.02%	96.60%	96.37%	93.98%	95.98%	95.84%	93.62%	95.55%	95.41%
0°C	Range [km]	117.04	151.13	151.12	119.32	138.95	138.69	119.1	129.37	126.38
	Efficiency	92.98%	96.21%	95.98%	92.96%	95.44%	95.28%	92.53%	94.82%	94.66%
−5°C	Range [km]	– *	148	148	–	136.16	136.15	–	119.85	119
	Efficiency	–	95.82%	95.59%	–	95.07%	94.90%	–	94.45%	94.33%

(*) The vehicle cannot follow reference speed due to drop of available power.

Table 4
Simulation results in case of half-used battery cells

		ECE15			Real cycle 1 (urban area)			Real cycle 2 (suburban area)		
		Battery	Hybrid (half-used UC cells)	Hybrid (fresh UC cells)	Battery	Hybrid (half-used UC cells)	Hybrid (fresh UC cells)	Battery	Hybrid (half-used UC cells)	Hybrid (fresh UC cells)
25°C	Range [km]	132.65	145.92	146.97	124.84	134.40	134.45	119.23	126.02	126.05
	Efficiency	94.75%	96.69%	96.91%	94.66%	96.12%	96.42%	94.37%	95.87%	96.03%
10°C	Range [km]	113.92	138.66	138.93	114.33	126.16	126.19	114.07	119.08	119.09
	Efficiency	93.28%	96.09%	96.30%	93.26%	95.38%	95.55%	92.90%	94.95%	95.12%
0°C	Range [km]	–	132.38	135.52	–	119.13	119.14	–	113.34	113.5
	Efficiency	–	95.62%	95.83%	–	94.74%	94.91%	–	94.16%	94.32%
−5°C	Range [km]	–	129.25	129.26	–	99.51%	99.73	–	111.42	111.45
	Efficiency	–	95.18%	95.41%	–	94.18%	94.44%	–	93.66%	93.84%

Results for four different ambient temperatures in the case of the fresh battery cells are presented in Table 3. The cell temperature increases due to self-heating during long drives even more than by 10°C. Hybridization effect on improving the performance of the vehicle is revealed by increased efficiency and range. An extended range of the vehicle with the hybrid source results not only from higher efficiency but also from smaller decrease in the capacity, because of smaller battery discharge currents. In the low temperature range deterioration of a battery power performance is so serious that the vehicle is not able to drive in accordance with the aforementioned driving cycles. This problem is solved by the hybrid source, where most of the power pulse is provided by the UCs. When vehicle is powered by the hybrid source, for urban cycles at the temperature of -5°C decrease in range is at the level of 10%. Even in the nominal conditions, i.e. in ECE15 cycle at 25°C, range is still 13km higher than for the battery source. A range reduction at 0°C is at the level of 22% for non-hybrid only battery-based propulsion whereas for the hybrid source it is only 8%. The results for half-used UCs show that the aging process of UCs does not significantly affect the performance. When replacing the batteries with new ones after few years of operation, there is no need to replace the UCs.

When battery is partially used up supporting by UCs is more substantial (Table 4). The increase of battery internal resistance (20%) causes significant deterioration in performance and available power. Simulation results clearly show that in this case hybridization is not only technically justified, but is essential to maintain the expected dynamics of a vehicle at low temperatures.

5. Conclusions

The benefits of the energy storage hybridization have been investigated quantitatively. Four examined case studies for the city BEV clearly show that supporting a high-energy storage with a high-power one in transient states noticeably enhances vehicle performance. Battery wear-down is caused by cycling and ageing. Most lithium-based chemistries are quite robust to shallow cycling. However, the shallow cycling with currents much above 0.5 C-rate during acceleration and regenerative deceleration has much lower efficiency than in case of ultracapacitors. The overall energy consumption per distance unit goes up if not supported with the high-power storage, and this in turn increases number of deep cycles needed to travel the same distance (e.g. per year). Additionally, some chemistries cannot deliver enough specific power if temperature drops below a certain level, which is typical e.g. for the central Europe climate. This means that the battery pack requires heating if operated without auxiliary high-power storage. If this heat is produced using energy stored in the battery, the range of a vehicle decreases and the number of cycles per year increases. It has been shown that ultracapacitors can significantly ex-

tend the temperature range in which such a hybrid source can deliver required power without additional battery heating system and regardless to ageing processes. The auxiliary storage does not present substantial packaging problems in the design of the vehicle. For studied case, mass of the $LiFePO_4$ cells is 140 kg and volume is 90 dm^3 [27]. The auxiliary storage adds less than 10% of batteries mass to the powertrain and its volume is ca. 14 dm^3 [28]. Despite the higher initial costs, a hybrid energy source may be profitable through extending lifetime and vehicle range as well as through preserving power capability under all conditions. After extensive simulation tests performed in Matlab/Simulink/Plecs environment it was decided that in the case of $LiFePO_4$ chemistry it is technically and economically justified to hybridize this storage with the help of ultracapacitors also in the case of a city car. The quantitative efficiency results complemented with cost, gravimetric and volumetric analysis convinced us to hybridize the energy storage for the ECO-Car we have been designing recently. Currently an experimental mobile mockup is being built.

Acknowledgements. The publication partly-financed by the European Union within the European Regional Development Fund (the ECO-Mobility project WND-POIG.01.03.01-14-154/09, 2009-2013).

REFERENCES

[1] A. Fuhs, *Hybrid Vehicles and the Future of Personal Transportation*, CRC Press, London, 2009.
[2] www.energybulletin.net/node/22381, "CERA (Cambridge Energy Research Associates) says peak oil theory is faulty", *Energy Bulletin*, 2006.
[3] G. Piastoia, *Electric and Hybrid Vehicles*, Elsevier Science Publishers, Amsterdam, 2010.
[4] L. Fulton, *Technology Roadmap: Electric and Plug-in Hybrid Electric Vehicles*, International Energy Agency, www.iea.org, updated June 2011.
[5] K. Umezu, H. Noyama, "Air-conditioning system for electric vehicles (i-MiEV)", *SAE Automotive Refrigerant & System Efficiency Symposium* 1, CD-ROM (2010).
[6] "From home to work, the average commute is 26.4 minutes", *OmniStats* 3 (4), 1–4 (2003).
[7] www.solarisbus.pl/en/hybrid,text,98.html (accessed on 15.01.2011).
[8] C. Liu, Z. Yu, D. Neff, A. Zhamu, and B.Z. Jang, "Graphene-based supercapacitor with an ultrahigh energy density", *Nano Letters* 10 (12), 4863–4868 (2010).
[9] K. Bullis, "Ultracapacitors to boost the range of electric cars", *Technology Review* 1, CD-ROM (2011).
[10] *Low Cost Graphene Electrode Powered Supercapacitors for Consumer Devices and EVs*, www.nanotune.com (accessed on December 2011).
[11] D.L. Chandler, "Research update: improving batteries' energy storage", *MIT News* 1, CD-ROM (2011).
[12] *Nanophosphate™ Lithium Ion Batteries*, www.a123systems.com (accessed on December 2011).
[13] L. Niedzicki, "Characterization of new generation of electrolytes based on imidazole derivatives salts", *Ph.D. Dissertation*, Warsaw University of Technology, Warszawa, 2010.
[14] A. Khaligh and Li Zhihao, "Battery, ultracapacitor, fuel cell, and hybrid energy storage systems for electric, hybrid electric, fuel cell, and plug-in hybrid electric vehicles: state of the art", *IEEE Trans. on Vehicular Technology* 59 (6), 2806–2814 (2010).
[15] S.M. Lukic, S.G. Wirasingha, F. Rodriguez, Jian Cao, and A. Emadi, "Power management of an ultracapacitor/battery hybrid energy storage system in an HEV", *IEEE Vehicle Power and Propulsion Conf.* 1, 1–6 (2006).
[16] A.M. Puscas, M.C. Carp, C.Z. Kertesz, P.N. Borza, and G. Coquery, "Thermal and voltage testing and characterization of supercapacitors and batteries", *IEEE 12th Int. Conf. on Optimization of Electrical and Electronic Equipment* 1, 125–132 (2010).
[17] T.P. Kohler, D. Buecherl, and H.-G. Herzog, "Investigation of control strategies for hybrid energy storage systems in hybrid electric vehicles", *IEEE Vehicle Power and Propulsion Conf.* 1, 1687–1693 (2009).
[18] I. Aharon and A. Kuperman, "Design of semi-active battery-ultracapacitor hybrids", *IEEE 26-th Convention of Electrical and Electronics Engineers in Israel* 1, 593–597 (2010).
[19] A. Kuperman and I. Aharon, "Battery–ultracapacitor hybrids for pulsed current loads: a review", *Renewable and Sustainable Energy Reviews* 15 (2), 981–992 (2011).
[20] M.B. Camara, H. Gualous, F. Gustin, and A. Berthon, "Design and new control of DC/DC converters to share energy between supercapacitors and batteries in hybrid vehicles", *IEEE Trans. on Vehicular Technology* 57 (5), 2721–2735 (2008).
[21] R.M. Miskiewicz and A.J. Moradewicz, "Contactless power interface for plug-in electric vehicles in V2G systems", *Bull. Pol. Ac.: Tech.* 59 (4), 561–568 (2011).
[22] L. Gao, S. Liu, and R. A. Dougal, "Dynamic lithium-ion battery model for system simulation", *IEEE Trans. on Components and Packaging* 25 (3), 495–505 (2002).
[23] M. A. Roscher, and D. U. Sauer, "Dynamic electric behavior and open-circuit-voltage modeling of $LiFePO_4$-based lithium ion secondary batteries", *J. Power Sources* 196 (1), 331–336 (2011).
[24] H.G. Schweiger, O. Obeidi, O. Komesker, A. Raschke, M. Schiemann, C. Zehner, M. Gehnen, M. Keller, and P. Birke, "Comparison of several methods for determining the internal resistance of Li-ion cells", *Sensors* 10 (6), 5604–5625 (2010).
[25] M. Michalczuk, L.M. Grzesiak, and B. Ufnalski, "A lithium battery and ultracapacitor hybrid energy source for an urban electric vehicle", *Electrotechnical Review* 88 (4B), 58–162 (2012).
[26] www.semikron.com, IGBT module datasheet SKM300GB-12T4 (accessed on 8.12.2011).
[27] http://en.winston-battery.com (accessed on 8.12.2011).
[28] www.maxwell.com, BC (BOOSTCAP) Series Datasheet (accessed on 8.12.2011).